

# Refill friction stir spot welding of AlSi10Mg alloy produced by laser powder bed fusion to wrought AA7075-T6 alloy



S. Fritsche<sup>a</sup>, J. Draper<sup>b</sup>, A. Toumpis<sup>b</sup>, A. Galloway<sup>b</sup>, S.T. Amancio-Filho<sup>a,\*</sup>

<sup>a</sup> Graz University of Technology, Institute of Materials Science, Joining and Forming, BMK Endowed Professorship for Aviation, Graz, Austria

<sup>b</sup> University of Strathclyde, Department of Mechanical & Aerospace Engineering, Glasgow, United Kingdom

## ARTICLE INFO

### Article history:

Received 8 July 2022

Received in revised form 16 September 2022

Accepted 17 September 2022

Available online 11 October 2022

### Keywords:

Refill Friction Stir Spot Welding

Additive manufacturing

Laser powder bed fusion

Aluminium alloys

Aerospace materials

## ABSTRACT

In this study, refill friction stir spot welding (RFSSW) was used to join AlSi10Mg, produced by laser powder bed fusion (LPBF), to high-strength wrought AA7075-T6 alloy. The investigation showed the best mechanical properties and integrity of the joint are achieved with medium heat input, where the optimal balance between hook height and integrity was observed. The welded additive manufactured alloy shows accentuated softening in the hook region of the thermo-mechanically affected zone. The feasibility of RFSSW for joining LPBF AlSi10Mg to high-strength wrought alloys was confirmed, showing high potential for further investigations and industrial applications.

© 2022 The Author(s). Published by Elsevier Ltd on behalf of Society of Manufacturing Engineers (SME). This is an open access article under the CC BY-NC-ND license (<http://creativecommons.org/licenses/by-nc-nd/4.0/>).

## 1. Introduction

AlSi10Mg is the most common aluminium alloy processed by laser powder bed fusion (LPBF) and the influence of process parameters on print quality is already well investigated [1,2]. Due to part size limitations related to the build chamber dimensions, it is often necessary to join LPBF printed parts. Solid-state welding techniques such as friction stir welding (FSW) have shown good weld quality and mechanical properties for AlSi10Mg alloy joints [3,4].

The refill friction stir spot welding (RFSSW) process [5] has garnered significant interest in recent years due to its solid-state nature and subsequent capability of joining metals that are not weldable with fusion-based processes. For use in the aviation and aerospace industries, the RFSSW of high-strength aluminium alloys offers a crucial lightweight replacement for rivets and screws [6], because no rivet heads or nuts are needed [5]. Therefore, joining AlSi10Mg parts to 2xxx or 7xxx series wrought alloys is of great interest. Besides investigations on different wrought aluminium alloys, recent studies in RFSSW have focused on dissimilar welds of these alloys with titanium, magnesium or steel [7–9]. In this study, the feasibility of joining LPBF produced AlSi10Mg alloy to wrought AA7075-T6 alloy was investigated. To the best of the

authors' knowledge, no prior research into the joining of LPBF printed alloys using RFSSW has been reported.

## 2. Materials and methods

Coupons with dimensions of 100 mm × 30 mm and thickness of 2 mm were joined in a lap joint configuration, with an overlap of 30 mm. LPBF printed AlSi10Mg and wrought AA7075-T6 were used as the top and bottom sheets, respectively. The AlSi10Mg coupons were printed with a Creator RA (Coherent, USA) LPBF equipment using optimized parameters (optimization study results available upon request). Associated printing parameters as well as the mechanical properties of the LPBF printed and wrought alloy are presented in Table 1.

The RPS100 RFSSW equipment (Harms & Wende, Germany) was used with a H13 steel commercial tool and outer diameters of 6.4 mm, 9 mm and 18 mm for probe, shoulder and clamping ring, respectively. The rotational speed was varied from 800 to 2200 rpm whereby lower rotational speed corresponds with lower heat input (HI). The plunge depth (PD), welding time (WT) and travel factor, representing the ratio of PD to maximum probe retraction, were kept constant at 2.5 mm, 4 s and 0.8 respectively. Temperature measurements were taken on the outside of the clamping ring (TC0) and in the interface between the coupons (TC1, TC2, attached to the AA7075-T6 coupon) using type K thermocouples. A TC0 temperature of 160 °C was established before

\* Corresponding author at: Institute of Materials Science, Joining and Forming, Graz University of Technology, Kopernikusgasse 24/I, 8010 Graz, Austria.

E-mail address: [sergio.amancio@tugraz.at](mailto:sergio.amancio@tugraz.at) (S.T. Amancio-Filho).

**Table 1**  
LPBF printing parameters for the AlSi10Mg and mechanical properties for the joined alloys.

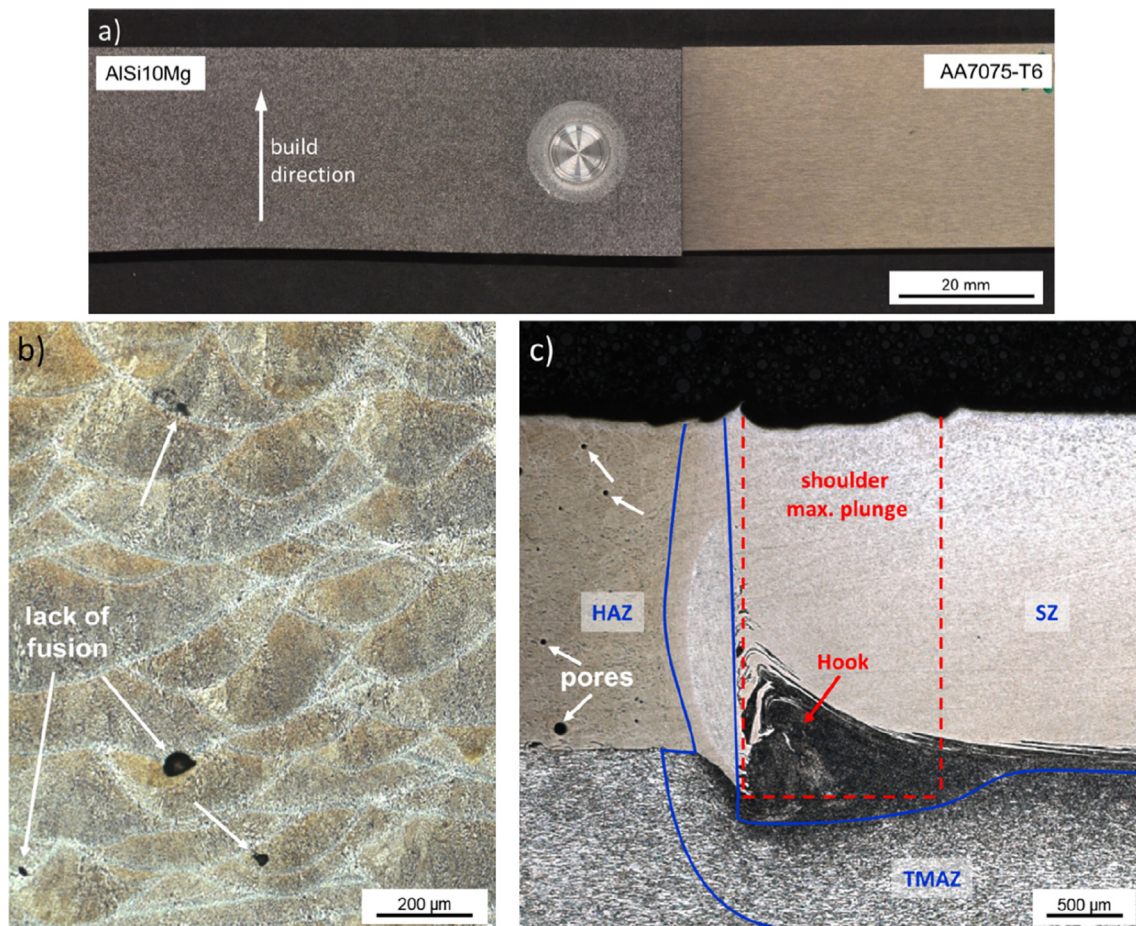
	Parameter	Value
LPBF process parameters	Layer thickness	20 $\mu\text{m}$
	Spot size diameter	140 $\mu\text{m}$
	Beam Expander Diameter	120 $\mu\text{m}$
	Laser power	240 W
	Contouring mark speed	810 mm/s
	Hatching mark speed	612 mm/s
AlSi10Mg as-built	Ultimate tensile strength	423 MPa
	Yield strength	255 MPa
	Elongation at break	8.3 %
	Hardness	124 HV
AA7075-T6	Ultimate Tensile Strength (UTS)	610 MPa
	Yield strength	545 MPa
	Elongation at break (A)	9.7 %
	Hardness	195 HV

starting a weld cycle. Lap-shear tests were carried out using a cross-head speed of  $2 \text{ mm min}^{-1}$  at room temperature following EN ISO 14273. The microstructure of the weld cross-sections was investigated using optical microscopy (OM) after a standard metallographic procedure and etching with Keller's reagent (95 ml  $\text{H}_2\text{O}$ , 1.5 ml HF, 1 ml HCl, 2.5 ml  $\text{HNO}_3$ ) for 14 s. Vickers HV0.05 microhardness mappings were obtained following EN ISO 6507.

### 3. Results and discussion

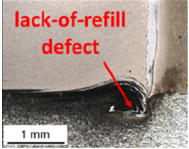
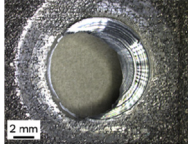
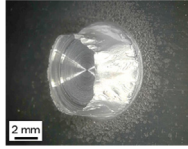
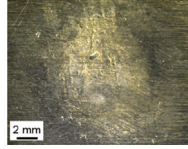
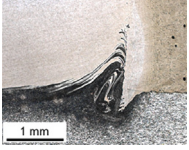
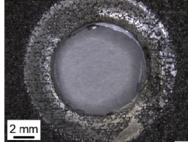
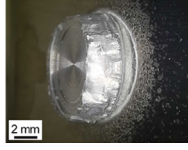
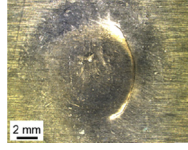
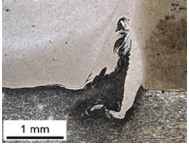
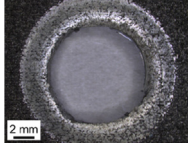
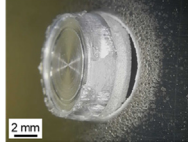
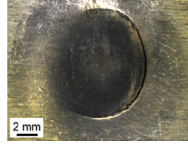
For all obtained parameters, good surface quality of the weld could be achieved (Fig. 1(a)), since no kissing-bond defects, voids

or lack of refill at the surface could be observed. LPBF-process related lack of fusion defects and pores in the AlSi10Mg could be identified in the as-built material (Fig. 1(b)) and in the heat-affected zone (HAZ) of the welded coupon (Fig. 1(c)). Due to sufficient mixing of the material in the stirr zone (SZ), no LPBF defects remain and in the thermo-mechanically affected zone (TMAZ) decreased porosity can be observed which is following the findings from Scherillo et al. [3]. Joints obtained with an RS of 1500 rpm (medium HI) and 2200 rpm (high HI) show complete refill unlike an RS of 800 rpm, where, due to lower heat input, lack of refill occurred in the area of the outer edge of the shoulder at maximum plunge depth. Similar defects due to insufficient material flow



**Fig. 1.** (a) RFSSW single-lap joint; (b) microstructure of AlSi10Mg in as-built condition and (c) of the hook region, different weld zones and the plunge area of a joint welded with RS of 1500 rpm (The centre of the spot weld is on picture's right-hand side).

**Table 2**  
Mean ultimate lap shear force, hook defect and fracture mode for different RS.

RS [rpm]	Mean ULSF [kN]	Hook	AlSi10Mg (TOP)	AA7075-T6 (TOP)	AA7075-T6 (BOTTOM)	Fracture Mode
800	9.01 ± 0.12					shear-plug
1500	9.16 ± 0.11					plug pull-out
2200	8.92 ± 0.09					plug pull-out

during refill were reported by De Castro et al. [10] and Kubit et al. [11]. For medium and high HI-welds, an area with coarse microstructure was observed next to the hook – a circumferential geometrical feature formed as a result of tool plunging and retraction – in the TMAZ of the AlSi10Mg (Fig. 1(c)). This suggests the presence of dynamic recrystallization and grain growth.

The mean ultimate lap shear force (ULSF) results in Table 2 show the best performance for RS of 1500 rpm. The achieved average ULSF of 9.16kN is in between the values obtained by Effertz

et al. [12] for AA7050-T76 and Silva et al. [13] for AA6082-T6 with 11.3kN and 8.5kN, respectively, using a probe diameter of 6 mm. A decrease in hook height was observed for all the performed joints when decreasing RS (Table 2). Cao et al. [14] stated that lower hook height leads to higher ULSF values. Moreover, lower RS (1000–1100 rpm) usually leads to better lap shear strength in high-strength aluminium alloys, as less extensive material plasticisation and mixing take place, leading to lower hook height [15–17]. This corresponds with the ULSF results for this work’s medium and high

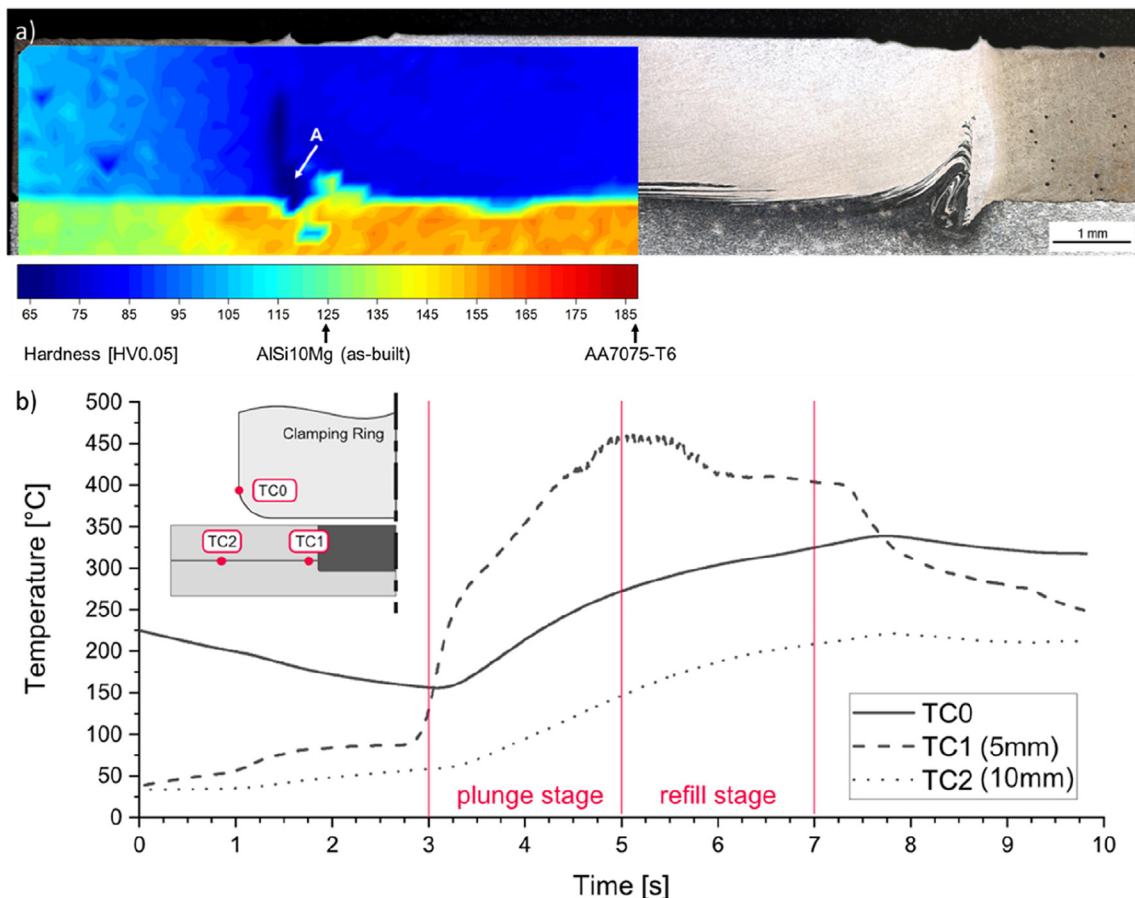


**Fig. 2.** RFSSW joint obtained with RS = 1500 rpm; (a) cross-section and Vickers hardness mapping and (b) temperature measurement.

HI-welds. For the low HI-welds, the lack-of-refill circumferential defect (resulting from insufficient material plasticisation) led to slightly lower ULSF. Furthermore, this circumferential defect had an influence on the fracture mode, as shown in Table 2. Shear-plug fracture mode was observed whereas middle and high HI-welds showed plug pull-out fracture mode. The detailed investigation on the influence of HI on ULSF and fracture mechanisms is out of the scope of this manuscript. These results will be provided in a separate publication.

The microhardness of the weld cross-section related to RS of 1500 rpm is displayed in Fig. 2(a). In comparison to the base materials, with a hardness of 124HV and 195HV for AlSi10Mg and AA7075-T6 respectively, a significant softening effect (i.e. a 33 % decrease in hardness) could be identified in the SZ of AlSi10Mg. This effect appears even greater in the hook region of the thermo-mechanically affected zone (TMAZ) (Fig. 2(a), A). Next to this softened area, coinciding with the coarse grain area observed by optical microscopy, a high local temperature of 450 °C (Fig. 2 (b)) was measured at the beginning of the refill stage. Therefore, it may be assumed that the local temperature in the softened zone is even higher at this point, supporting local annealing.

In contrast to the increase in hardness with increasing distance from the SZ in the upper sheet, a further decrease could be observed in the lower sheet, although hardness in the wrought alloy is still higher than in the printed AlSi10Mg. The minimum hardness in the HAZ of the AA7075 is typical for precipitation-hardenable aluminium alloys because coarse precipitates lead to the over-ageing of the material [18]. The measured temperatures in the lower sheet at a distance of 10 mm from the weld centre (TC2), and on the outside of the clamping ring (TC0) increase constantly throughout welding, reaching local peak temperatures of 220 °C and 340 °C, respectively.

#### 4. Conclusions

RFSSW has been successfully performed on a dissimilar joint of LPBF processed AlSi10Mg and wrought AA7075-T6. A reduction in LPBF-process related porosity was observed in the SZ and TMAZ. A zone with accentuated softening formed next to the hook in the TMAZ of the LPBF printed AlSi10Mg and is related to the high peak temperatures, measured at the beginning of the refill stage. Medium heat input welds showed the best balance between low hook height and weld integrity and consequently demonstrated the best lap-shear performance. Lowering the hook height by decreasing the heat input, i.e. lowering RS, was achieved, hence it is expected that ULSF can be increased at lower-to-medium heat inputs by optimizing the material flow during the refill stage to avoid the formation of circumferential lack of refill defects.

#### Declaration of Competing Interest

The authors declare that they have no known competing financial interests or personal relationships that could have appeared to influence the work reported in this paper.

#### Acknowledgements

The authors gratefully acknowledge financial support from the Austrian aviation program “TAKE OFF” (PILOT, Grant No. 852796,

2018) and BMK—The Austrian Ministry for Climate Action, Environment, Energy, Mobility, Innovation and Technology. The authors would like to acknowledge Magna Steyr Fahrzeugtechnik AG & Co KG for providing the joining equipment, AMAG Austria Metall AG for the base material, and the Open Access Funding by Graz University of Technology.

#### References

- [1] Zhang J, Song B, Wei Q, Bourell D, Shi Y. A review of selective laser melting of aluminum alloys: Processing, microstructure, property and developing trends. *J Mater Sci Technol* 2019;35(2):270–84. <https://doi.org/10.1016/j.jmst.2018.09.004>.
- [2] Thijs L, Kempen K, Kruth JP, Van Humbeeck J. Fine-structured aluminium products with controllable texture by selective laser melting of pre-alloyed AlSi10Mg powder. *Acta Mater* 2013;61(5):1809–19. <https://doi.org/10.1016/j.actamat.2012.11.052>.
- [3] Scherillo F et al. Friction Stir Welding of AlSi10Mg Plates Produced by Selective Laser Melting. *Metallogr Microstruct Anal* 2018;7(4):457–63. <https://doi.org/10.1007/S13632-018-0465-Y/TABLES/2>.
- [4] Du Z, Tan MJ, Chen H, Bi G, Chua CK. Joining of 3D-printed AlSi10Mg by friction stir welding. *Weld World* 2018;62(3):675–82. <https://doi.org/10.1007/S40194-018-0585-7>.
- [5] Schilling U, dos Santos J. Method and device for joining at least two adjoining work pieces by friction welding US672256B2, 2004.
- [6] Feng XS, Bin Li S, Tang LN, Wang HM. Refill Friction Stir Spot Welding of Similar and Dissimilar Alloys: A Review. *Acta Metall Sin (English Lett.)* 2020; 33(1): 30–42. doi: 10.1007/S40195-019-00982-4/FIGURES/17.
- [7] Plaine AH, Gonzalez AR, Suhuddin UFH, dos Santos JF, Alcântara NG. The optimization of friction spot welding process parameters in AA6181-T4 and Ti6Al4V dissimilar joints. *Mater Des* 2015;83:36–41. <https://doi.org/10.1016/j.matdes.2015.05.082>.
- [8] Suhuddin U, Fischer V, Kroeff F, dos Santos JF. Microstructure and mechanical properties of friction spot welds of dissimilar AA5754 Al and AZ31 Mg alloys. *Mater Sci Eng A* 2014;590:384–9. <https://doi.org/10.1016/j.msea.2013.10.057>.
- [9] Dong H, Chen S, Song Y, Guo X, Zhang X, Sun Z. Refilled friction stir spot welding of aluminum alloy to galvanized steel sheets. *Mater Des* 2016;94:457–66. <https://doi.org/10.1016/j.matdes.2016.01.066>.
- [10] de Castro CC, Plaine AH, de Alcântara NG, dos Santos JF. Taguchi approach for the optimization of refill friction stir spot welding parameters for AA2198-T8 aluminum alloy. *Int J Adv Manuf Technol* 2018;99(5–8):1927–36. <https://doi.org/10.1007/s00170-018-2609-2>.
- [11] Kubit A, Kluz R, Trzepieciński T, Wydrzyński D, Bochnowski W. Analysis of the mechanical properties and of micrographs of refill friction stir spot welded 7075-T6 aluminium sheets. *Arch Civ Mech Eng* 2018;18(1):235–44. <https://doi.org/10.1016/j.acme.2017.07.005>.
- [12] Effertz PS, Quintino L, Infante V. The optimization of process parameters for friction spot welded 7050–T76 aluminium alloy using a Taguchi orthogonal array. *Int J Adv Manuf Technol* 2017;91(9–12):3683–95. <https://doi.org/10.1007/s00170-017-0048-0>.
- [13] Silva BH, Zepón G, Bolfarini C, dos Santos JF. Refill friction stir spot welding of AA6082-T6 alloy: Hook defect formation and its influence on the mechanical properties and fracture behavior. *Mater Sci Eng A* 2020;773:.. <https://doi.org/10.1016/j.msea.2019.138724>.
- [14] Cao JY, Wang M, Kong L, Zhao HX, Chai P. Microstructure, texture and mechanical properties during refill friction stir spot welding of 6061–T6 alloy. *Mater Charact* 2017;128:54–62. <https://doi.org/10.1016/j.matchar.2017.03.023>.
- [15] Li Z, Ji S, Ma Y, Chai P, Yue Y, Gao S. Fracture mechanism of refill friction stir spot-welded 2024–T4 aluminum alloy. *Int J Adv Manuf Technol* 2016;86(5–8):1925–32. <https://doi.org/10.1007/s00170-015-8276-7>.
- [16] de Sousa Santos P, McAndrew AR, Gandra J, Zhang X. Refill friction stir spot welding of aerospace alloys in the presence of interfacial sealant. *Weld World* 2021;65(8):1451–71.
- [17] de Barros PAF, Campanelli LC, Alcântara NG, Dos Santos JF. An investigation on friction spot welding of AA2198-T8 thin sheets. *Fatigue Fract Eng Mater Struct* 2017;40(4):535–42. <https://doi.org/10.1111/ffe.12512>.
- [18] Zhao Y, Dong C, Wang C, Miao S, Tan J, Yi Y. Microstructures evolution in refill friction stir spot welding of al-zn-mg-cu alloy. *Metals (Basel)* 2020;10(1):145. <https://doi.org/10.3390/met10010145>.